

G. N. Abramovich, T. A. Girshovich,
and A. N. Grishin

UDC 532.525.2

A method is proposed for calculating the rarefaction occurring in the reverse-flow zone behind a jet ejected from an infinitely long slit at a right angle to a flow bounded by the walls of a channel. The calculated results are compared with experimental data.

Jets which develop in a confined entraining flow are encountered in different types of equipment and are particularly widely used to organize mixing in different types of mixers. When the jet is discharged into a transverse flow, the pressure in the region behind the jet is lower than the pressure in the incoming flow. This has an effect on the characteristics of the jet and especially on its path. It therefore also affects the depth of penetration of the jet, which in turn has a significant effect on the degree of mixing.

The problem of the rarefaction in the reverse-flow zone was solved in [1] for a plane jet in an infinite entraining flow. The main idea behind this solution was the use of the momentum equation in a projection normal to the entraining flow: since the pressure far above the jet is equal to the pressure in the undisturbed flow and there is no vertical projection of momentum (the jet practically rotates in the flow direction — see Fig. 1a), the increase in pressure in front of the jet on the wall from which it is discharged and the momentum of the jet should be compensated for by the rarefaction behind the jet.

To determine the integral of pressure on the wall ahead of the jet and the velocity and pressure on its front boundary, it is necessary to know the form of the "displacement body" formed by the jet. Based on the fact that the jet must again become attached to the wall to ensure closure of the circulation zone, it was assumed in [1] that this "displacement body" has the form of an ellipse. Thus, it is necessary to find three quantities: the pressure in the reverse-flow zone behind the jet, and two parameters determining the form of the ellipse — its semimajor and semiminor axes.

As the second and third equations to determine these quantities we used the conditions of transverse equilibrium at the nozzle edge and at a distance from the jet source in the region of minimum curvature of the "displacement body" — at the point of intersection of the curve of the ellipse with its semiminor axis. Since the pressure gradient is proportional to the square of the mean velocity in the jet in this section (which is less than the velocity of the entraining flow) and is inversely proportional to the radius of curvature, then from the condition of transverse equilibrium we find that the pressures above the jet in the region of minimum curvature of the displacement body and under it should be close to each other. The results of calculation of rarefaction behind a plane jet and the jet path obtained by the above-described method agree quite satisfactorily with the experimental data.

Below we present a solution to the problem of determining the rarefaction behind a plane jet in a confined entraining flow. The solution is based on the solution in [1] for a jet in an infinite entraining flow. Here, we make the following assumptions: 1) the flow outside the jet is a potential flow; 2) the pressure in the reverse-flow zone behind the jet is constant; 3) the displacement body formed by the jet has the form of an ellipse; 4) the direction of the velocity in the jet away from the source is close to the direction of the flow; 5) friction on the channel walls is absent. Given these assumptions, the flow of the jet in the channel can be obtained from the transverse potential flow past a grid of elliptical cylinders. The walls in this case play the role of streamlines. One of the walls and its extension coincides with the cylinder axis, while the other wall is the symmetry axis between two adjacent elliptical cylinders. As the contour of the displacement body we chose the dividing streamline — the line of constant flow rate separating the initial mass of the jet

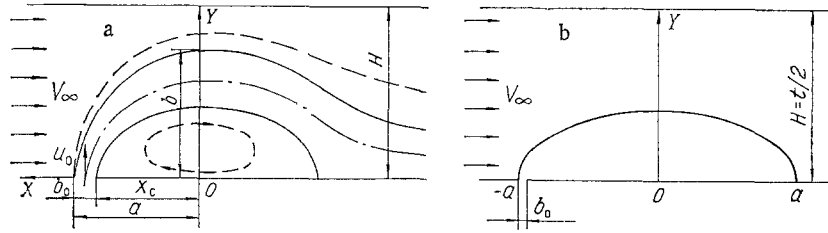


Fig. 1. Diagram of the flow (a) and the chosen design diagram (b).

from the apparent additional mass. In contrast to the contour of the displacement body in [1], this line is impermeable.

To determine the rarefaction behind the jet and the form of the displacement body, we can use the same three equations as in [1]:

$$\int_{-a}^a (p_1 - p_2) dx - \int_{-a}^0 p_2 dx + \frac{p_a + p_0}{2} b_0 + p_0 x_c + \rho_0 u_0^2 b_0 = 0, \quad (1)$$

$$\frac{p_a - p_0}{b_0} = \rho_0 \frac{u_0^2}{R_0}, \quad p_0 \approx p_{00}. \quad (2)$$

With allowance for assumption 3), the radius of curvature at the nozzle edge can be put equal to

$$R_0 = b^2/a. \quad (3)$$

In the case of discharge of the jet at a right angle to the flow bounded by the channel walls, only the flow conditions of the jet change, i.e., the characteristics of the entraining flow at the boundaries of the displacement body and the chosen contour.

Figure 1 shows the physical pattern of flow and the chosen flow scheme. It should be noted that in reality the dividing line of the stream shown in Fig. 1a is not a closed curve. Thus, the form of the rear part of the displacement body is not elliptical. However, since the chosen contour contains only the front part of the displacement body, this discrepancy can be ignored.

The flow characteristics in the channel were determined by using the results in [2], in which flow past a grid of cylinders close to elliptical in form was determined by conformal mapping of a grid of circles of unit radius onto the exterior of a grid of contours which were close to elliptical in form. The difference in the integrals of the pressure forces on the bottom and top walls of the channel was found to be equal to

$$I_x = \frac{1 - a_0^2}{a_0} I_{x1} - \frac{(1 - a_0)^2}{a_0} I_{x2}, \quad (4)$$

where

$$I_{x1} = R_0 \frac{\operatorname{ch} 2k - \cos 2k\lambda_1}{2k \sin 2k\lambda_1} \left(\frac{\pi}{2} - \arcsin \frac{1 - \cos 2k\lambda_1 \operatorname{ch} 2k}{\operatorname{ch} 2k - \cos 2k\lambda_1} \right);$$

$$I_{x2} = R_0 \frac{\operatorname{ch} 2k - \cos 2k\lambda_1}{2k \sqrt{1 - D_0^2}} \left(\frac{\pi}{2} + \arcsin \frac{1 - D_0 \operatorname{ch} 2k}{\operatorname{ch} 2k - D_0} \right) \quad \text{at } D_0^2 < 1;$$

$$I_{x2} = R_0 \frac{\operatorname{ch} 2k - \cos 2k\lambda_1}{2k \sqrt{D_0^2 - 1}} \ln \left(- \frac{D_0 - 1 + \sqrt{D_0^2 - 1} \operatorname{th} k}{D_0 - 1 - \sqrt{D_0^2 - 1} \operatorname{th} k} \right) \quad \text{at } D_0^2 > 1;$$

$$D_0 = a_0 (\operatorname{ch} 2k - \cos 2k\lambda_1) + \cos 2k\lambda_1, \quad k = \pi R_0/t, \quad \lambda_1 = \lambda/R_0,$$

R_0 is the radius of the circle; t is the mesh of the grid; λ is half the length of a segment on which dipoles of equal moment are distributed; a_0 is a parameter of the mapping function.

After we calculate the integrals of the pressure distribution on the bottom wall in front of the jet and on the top wall and then insert them into Eq. (1), we obtain a system of transcendental equations. This system was solved for the rarefaction on a computer

$$\Delta p = 2(p_\infty - p_0)/\rho_\infty V_\infty^2 . \quad (5)$$

It was also solved for the parameters α and b . The results in [2] were also used to compute the velocity and pressure distributions on the contour of the ellipse. These distributions can be used as boundary conditions to solve the problem of the flow characteristics in the jet by means of the formulas:

$$u_s = |\bar{\Phi}(z)|, \quad \bar{\Phi}(z) = \frac{\bar{\Phi}(\zeta)}{1 - a_0 + a_0 \bar{\Phi}(\zeta)}, \quad \bar{\Phi}(\zeta) = 1 - \frac{\operatorname{ch} 2k - \cos 2k\lambda_1}{\operatorname{ch} 2k\zeta - \cos 2k\lambda_1}. \quad (6)$$

Here, the relationship between the coordinates ζ and z has the form:

$$z = \zeta + a_0 F_1(\zeta), \quad F_1(\zeta) = i \frac{\operatorname{ch} 2k - \cos 2k\lambda_1}{2k \sin 2k\lambda_1} \ln \frac{\operatorname{sh} k(\zeta - i\lambda_1)}{\operatorname{sh} k(\zeta + i\lambda_1)}. \quad (7)$$

It should be noted that the above formulas give the solution found in [1] in the case of an unlimited increase in the mesh of the grid of ellipses.

Figure 2a shows results of calculation of the rarefaction behind a jet Δp in relation to the ratio of the dynamic heads of the jet and flow $q = \rho_0 u_0^2 / \rho_\infty V_\infty^2$ with different degrees of confinement of the entraining flow, i.e., different ratios of the height of the channel to the width of the slit from which the jet is ejected H/b_0 . It is apparent that rarefaction increases with an increase in q for a specified ratio H/b_0 . Here, the lower the value of H/b_0 , the more intensive its increase. A reduction in H/b_0 leads to a substantial increase in the rarefaction behind the jet.

Figure 2b shows the dependence of the rarefaction behind the jet on the same parameters, but the value of the rarefaction is referred not to the velocity at the channel inlet but instead to the mean flow velocity at the narrowest place above the jet u_{av} . It is apparent that the relative rarefaction changes negligibly with a change in q for a given value of H/b_0 . It can also be seen from the graph that the relative rarefaction, as determined above, is close to unity and does not change appreciably with a change in the degree of confinement of the entraining flow.

We similarly found that an increase in confinement of the flow (a decrease in H/b_0) leads to greater curvature of the contour of the displacement body and, thus, greater curvature of the path of the jet. It was also established that with a specified degree of confinement of the flow, the increase in pressure on the bottom wall of the channel in front of the jet depends little on the ratio of the dynamic heads of the jet and flow. However, this ratio has a substantial effect on the pressure distribution on the top wall of the channel: an increase in the parameter q is accompanied by an increase in rarefaction on the wall, with a change in q from 20 to 100 producing a more than threefold increase in rarefaction.

To check the above method of calculating rarefaction behind the jet, jet path, and pressure distribution on the channel walls, we compared the calculated results with experimental data obtained by studying a plane jet propagating in an entraining flow bounded by the walls of a channel.

The experiment was conducted with a special unit which included a wind tunnel with an outlet diameter of 200 mm. A sufficiently uniform flow with a low degree of turbulence was created (flow nonuniformity within the working section did not exceed 2%, while turbulence intensity did not exceed 1.5%). The working section in the experiment was a channel with a movable top wall. The inclusion of an ejector extension in this wall prevented spreading of the streamlines before entry of the jet. The channel was throttled with a small jet of air. To determine the coaxiality of the working section and the wind tunnel, the horizontal and vertical inlet edges of the channel were made in the form of wedges with holes on their generatrices to measure static pressure. A jet was injected into the channel from plane slits in the bottom wall (the subjacent surface). Limiting rings were installed at the sides of the slits to minimize flow of the air across the channel. The thickness of the boundary layer on the top and bottom walls ahead of the jet was no greater than 0.5 mm. The pressure distribution on the top and bottom walls of the channel was measured by means of 0.8-1-mm-diameter drain holes.

The measurements showed that there is an isobaric region with reduced pressure on the subjacent surface behind the jet. The pressure in this region later increases and approaches the atmospheric pressure but remains somewhat below it due to the supplying of additional mass into the jet and the presence of the ejector extension, at the outlet of which pressure is

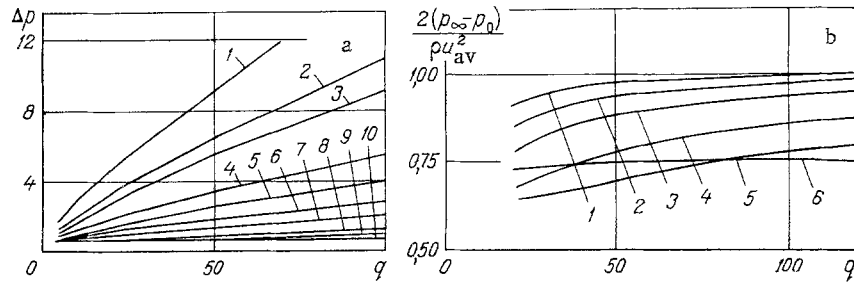


Fig. 2. Rarefaction behind a plane jet in a confined entraining flow: a) $\Delta p = 2(p_\infty - p_0) / \rho_\infty V_\infty^2$ [1) $H/b_0 = 25$; 2) 40; 3) 50; 4) 100; 5) 150; 6) 250; 7) 500; 8) 1250; 9) 2500; 10) 5000]; b) $\Delta \bar{p} = 2(p_\infty - p_0) / \rho u_{av}^2$ [1) $H/b_0 = 25$; 2) 50; 3) 100; 4) 250; 5) 500; 6) ∞].

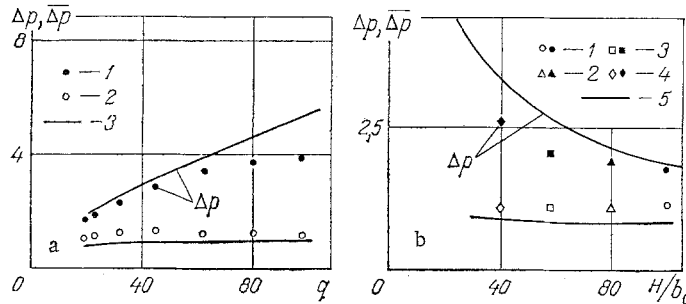


Fig. 3. Comparison of calculated and experimental data on rarefaction behind a plane jet in a confined entraining flow: a) 1 - Δp ; 2 - $\Delta \bar{p}$; $H/b_0 = 100$; 3 - theory; b) 1 - $q = 23.0$; 2 - 23.2; 3 - 17.9; 4 - 19.3; 5 - theory, $q = 20$.

equal to atmospheric. We took the rarefaction in the middle of the circulation zone as the rarefaction behind the jet in the tests. The length of the circulation zone in turn was determined as the distance from the rear edge of the nozzle to the point along the subjacent surface at which the excess rarefaction was equal to 0.05 of the maximum excess rarefaction in the reverse-flow zone $\Delta p - \Delta p_e = 0.05 (\Delta p_m - \Delta p_e)$, where Δp_e is the rarefaction at the end of the channel.

Figure 3 compares the results of calculation of the relation for rarefaction behind the jet with the above-described experimental data. It is apparent that the calculated results agree qualitatively and to a certain extent quantitatively with the test data.

Figure 4a shows jet paths with $H/b_0 = 100$ and two values of the ratios of the dynamic heads of the jet and the flow. The calculated jet paths were determined by means of the displacement-body contours found by the method described previously. As was already noted, it was reasoned that the contour of the displacement body is formed by the dividing streamline - the line of constant flow rate of the stream, which separates the initial mass of the jet from its apparent additional mass resulting from ejection. It should be noted that the thus-chosen displacement-body contour is impermeable, since it is bounded by a streamline. We used a normal to this line to plot the calculated ordinate of the dividing line of the stream in coordinates connected with the jet axis, y_p . The line $y_p = f(x)$, where x and y are curvilinear coordinates connected with the jet axis, can be determined from the condition of constancy of the flow rate in the part of the jet toward the flow bounded by the jet axis and the line $y_p = f(x)$. The experimental path of the jet was determined as the line of maximum velocities.

Figure 4b shows jet paths with similar values of the dynamic heads and with two degrees of flow confinement H/b_0 .

It is apparent from the graphs that the agreement between the theoretical and empirical data is quite satisfactory except for the case of strong ejection $q = 97.6$. In this case, there is considerable overlap of the channel (more than 75%) and anomalous behavior of the

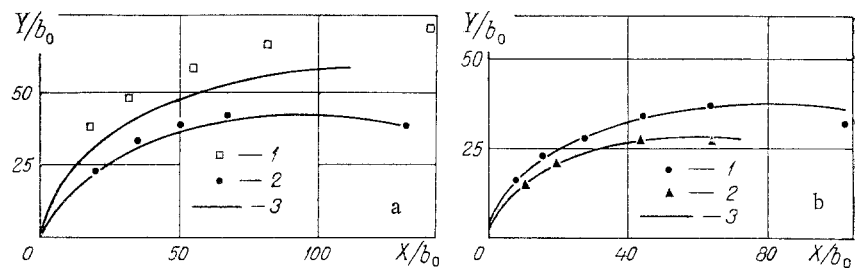


Fig. 4. Comparison of calculated and experimental data on jet path in a confined entraining flow: a) 1 - $q = 97.6$; 2 - 31.7; $H/b_0 = 100$; 3 - theory; b) 1 - $H/b_0 = 80$; $q = 37.6$; 2 - 54.4 and 36.7; 3 - theory.

experimental pressure distribution on the channel walls and the experimental circulation-zone length.

Thus, the proposed method of calculating rarefaction behind a plane jet developing in a transverse flow bounded by the walls of a channel and of predicting the path of the jet can be used in approximate calculations.

NOTATION

a , b , semimajor and semiminor axes of the ellipse; b_0 , width of the slit from which the jet is ejected; H , channel height; p_1 , p_2 , pressures on the bottom and top walls of the channel; p_a , p_0 , pressures directly ahead of the jet and in the reverse-flow zone behind the jet; $p\delta_0$, pressure at the boundary of the displacement body at $x = 0$; q , ratio of the dynamic heads of the jet and flow; R_0 , radius of curvature of the jet at the nozzle edge; u_0 , mean exit velocity of the jet; V_∞ , velocity of the entraining flow; x , y , curvilinear coordinates; x is directed along the jet axis, y is directed perpendicular to x ; y_p , dividing line of the stream; Δp , rarefaction in the reverse-flow zone behind the jet; ρ_0 , ρ_∞ , densities of the gas of the jet and entraining flow.

LITERATURE CITED

1. G. N. Abramovich and T. A. Girshovich, "Rarefaction behind a plane jet propagating in a transverse flow," *Izv. Akad. Nauk SSSR, Energ. Transp.*, No. 6, 113-118 (1984).
2. E. L. Blokh, "Study of a plane grid composed of theoretical profiles of finite thickness," *Tr. TsAGI*, No. 611 (1947).